

## New variational solution for the lowest subband level of the two-dimensional electron gas

A. A. Grinberg

*Department of Electrical Engineering, University of Minnesota, Minneapolis, Minnesota 55455*

(Received 25 January 1985)

An analytical formula for the first-subband energy level of the two-dimensional electron gas was derived using the variational method. Two different trial envelope wave functions were used: an Airy function with one variational parameter and an exponential-power function with two variational parameters. Solutions were obtained in the spherical effective-mass approximation with the envelope wave function assumed to vanish at the surface (or interface). In both cases we obtained quantitative agreement with the numerical self-consistent results within accuracies of 1% to 2% not only for the values of the first-subband energy but also for the average characteristics of the wave function. The accuracy of these solutions is several times better than the well-known variational solution proposed by F. F. Fang and W. E. Howard [Phys. Rev. Lett. 16, 797 (1966)]. Exchange-correlation energy is calculated in the local-density-functional approximation. Analytical form of this energy is obtained to first order of the perturbation theory using exponential-power variational wave function.

### I. INTRODUCTION

Studies of the energy levels of the two-dimensional electron gas (2DEG) using analytical<sup>1-3</sup> and numerical<sup>3-7</sup> approaches have been published in a number of papers. In spite of the fact that analytical methods have less accuracy because of the need to make some simplifying assumptions, they are more important, because they can be used in a number of other problems, such as those of electron scattering and optical transitions.

In the effective-mass approximation the simplest analytical solution of the problem can be obtained when the potential energy of the electron is considered as a triangular well. In this case the wave function of an electron is described by the Airy function  $Ai(\xi)$  in the form

$$\Psi(\mathbf{r}, z) = u(\mathbf{r}, z)\zeta(z) \exp(i\mathbf{k} \cdot \mathbf{r}), \quad (1.1)$$

where

$$\zeta(z) = \zeta_{tr}(z) = \alpha^{1/2} \frac{Ai(\xi)}{|Ai'(-\gamma)|} \quad (1.2)$$

is the envelope part of the wave function (tr indicates that it is triangular),

$$\xi = \alpha \left[ z - \frac{\gamma}{\alpha} \right], \quad (1.3)$$

$z$  is the coordinate along the axis perpendicular to the two-dimensional layer ( $z \geq 0$ ),  $\mathbf{r}$  is the two-dimensional coordinate vector, and  $\mathbf{k}$  the wave vector, both vectors being in the plane of the 2DEG,  $u(\mathbf{r}, z)$  is the Bloch function at the bottom of the conduction band,  $Ai'(\xi)$  is the derivative of  $Ai(\xi)$ , and  $\gamma$  is a root of the equation

$$Ai(-\gamma) = 0. \quad (1.4)$$

Equation (1.4) follows from the boundary condition  $\Psi = 0$  at the surface of the vertical wall of the potential well located at  $z = 0$ .

The parameter  $\alpha$  and the energy of the bottom subband  $E$  are related to the electric field  $F_0 = F_0(0+)$  by the equations

$$\alpha = \alpha_{tr} = (2meF_0/\hbar^2)^{1/3}, \quad (1.5)$$

$$E = E_{tr} = \gamma(\hbar^2/2m)^{1/3}(eF_0)^{2/3},$$

where  $e$  and  $m$  are the electron charge and the effective mass, respectively, and  $\gamma = 2.338$  is the smallest root of Eq. (1.4).<sup>8</sup> As can be seen from Eq. (1.5), this root defines the lowest energy level  $E$  which will be the main interest of this paper.

Other properties of the solution, no less important than the energy, are the average separation of carriers in the subband from the surface of the vertical potential well ( $Z_1$ ), defined as the average value of the coordinate  $z$  associated with the wave function  $\zeta(z)$  and the average value of  $z^2$  ( $Z_2$ ) given by Ref. 3

$$Z_1 = Z_{1,tr} = \int_0^\infty z |\zeta(z)|^2 dz = 2\gamma/3\alpha_{tr}, \quad (1.6)$$

$$Z_2 = Z_{2,tr} = \frac{8}{15}(\gamma/\alpha_{tr})^2.$$

In practice the electric field is not constant in the region of the 2DEG. Nevertheless, if the surface concentration of the 2DEG,  $n_s$  is substantially less than the number of impurity charges per unit area in the depletion layer  $N_{depl}$  (in the case when the two-dimensional gas forms near the heterointerface,  $N_{depl}$  is the number of impurity charges in the depletion layer on the side of 2DEG localization) the electric field can be considered constant for distances of the order of the size of the wave function ( $1/\alpha$ ) and equals  $F_0 = F(0+) = (4\pi e/\epsilon)(N_{depl} + n_s)$ , where  $\epsilon$  is the dielectric constant in the region of the 2DEG.

Then we have

$$\tilde{\alpha}_{\text{tr}} = 2\pi^{1/3}(\tilde{N}_{\text{depl}} + \tilde{n}_s)^{1/3}, \quad (1.7)$$

$$\tilde{E}_{\text{tr}} = 4\gamma\pi^{2/3}(\tilde{N}_{\text{depl}} + \tilde{n}_s)^{2/3}.$$

In Eq. (1.7) and below we will use the tilde to indicate energy in units of the effective Bohr energy  $E_B = \hbar^2/2mR_B^2$  and other values for which the unit length is the effective Bohr radius  $R_B = \epsilon\hbar^2/me^2$ .

The main shortcoming of the triangular approximation is that it does not take into account the influence of the self-consistent field of electrons on the single-particle potential.

A more accurate solution for the lowest subband of the 2DEG was derived by Fang and Howard<sup>1</sup> using the variational method with a trial envelope eigenfunction of the form

$$\zeta_{\text{FH}}(z) = \alpha \left( \frac{\alpha}{2} \right)^{1/2} z \exp \left[ -\frac{\alpha z}{2} \right], \quad (1.8)$$

where  $\alpha$  is the variational parameter.

To first order in the parameter

$$\lambda = R_B^{1/3} N / (N_{\text{eff}})^{4/3}, \quad (1.9)$$

where  $N$  is a volume concentration of ionized impurity centers in the depletion region,  $N_{\text{eff}} = N_{\text{depl}} + \frac{11}{32}n_s$ ,  $N_{\text{depl}} = NL$  and  $L$  is the depletion-region width (on the side of the 2DEG); the value of  $\alpha$  is given by<sup>3</sup> (FHS denotes the Fang-Howard-Stern approximation)

$$\tilde{\alpha} = \tilde{\alpha}_{\text{FHS}} = 2(6\pi\tilde{N}_{\text{eff}})^{1/3} - \frac{4\tilde{N}}{3\tilde{N}_{\text{eff}}}. \quad (1.10)$$

The parameter  $\lambda$  describes the influence of the potential curvature of the depletion-charge density. As was pointed out in Reg. 3,  $\lambda$  will be small in a Si inversion layer because the latter is generally much thinner than the depletion-layer width. The same will be true in the case of the AlGaAs-GaAs 2DEG.

In Eq. (1.10) and below it is assumed that only the first subband is occupied.

Within the same accuracy as in Eq. (1.10) the energy of the bottom of the first subband is given by<sup>3</sup>

$$\begin{aligned} \tilde{E}_{\text{FHS}} = & 3\pi^{2/3}(36/\tilde{N}_{\text{eff}})^{1/3} \left[ \tilde{N}_{\text{depl}} + \frac{55\tilde{n}_s}{96} \right] \\ & - 2(6\pi)^{1/3}\tilde{N} \frac{\tilde{N}_{\text{depl}} + (11\tilde{n}_s/96)}{\tilde{N}_{\text{eff}}^{5/3}}. \end{aligned} \quad (1.11)$$

The values  $Z_1$  and  $Z_2$  in this case are equal to

$$Z_{1,\text{FHS}} = 3/\alpha_{\text{FHS}}, \quad Z_{2,\text{FHS}} = 12/\alpha_{\text{FHS}}^2. \quad (1.12)$$

In Figs. 1(a) and 2(a) the ratios  $E_{\text{tr}}/E_{\text{FHS}}$ ,  $Z_{1,\text{tr}}/Z_{1,\text{FHS}}$  are plotted as functions of  $n_s/N_{\text{depl}}$ . At low concentration of the 2DEG the value  $E_{\text{tr}}/E_{\text{FHS}}$  approaches 0.944;

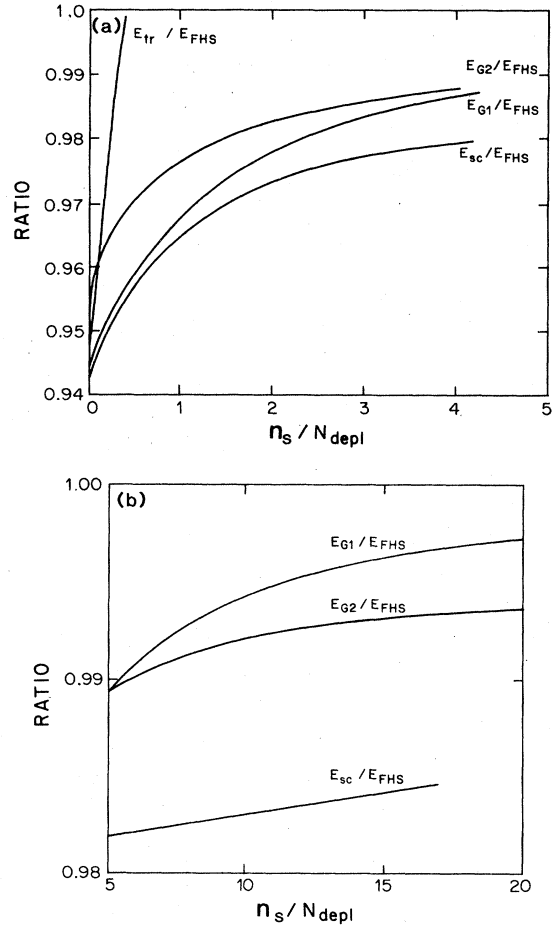


FIG. 1. Ratios of self-consistent ( $E_{\text{sc}}$ ), triangular-potential approximation ( $E_{\text{tr}}$ ), Airy trial function ( $E_{\text{G1}}$ ), and trial function (4.1) ( $E_{\text{G2}}$ ) values of the energy of the lowest subband to the energy  $E_{\text{FHS}}$  which follows from the trial function (1.8), as functions of the ratio of the two-dimensional electron-gas concentration ( $n_s$ ) to the depletion-layer impurity concentration ( $N_{\text{depl}}$ ).

however, with the increase of  $n_s$  it exceeds  $E_{\text{FHS}}$  by more than 15% as can be seen from Eqs. (1.7) and (1.11). The average separation of the electron charge is also different for these two solutions. At low  $n_s$  the value  $Z_{1,\text{tr}}/Z_{1,\text{FHS}}$  goes to 0.94, but for  $n_s \gg N_{\text{depl}}$  it is equal to 0.66. We will see which wave function gives a better approximation by comparing them with the numerical self-consistent result given by Stern.<sup>3</sup>

Section II gives the basic equations that have to be solved in the variational approach. In Sec. III we calculate the subband energy using the trial function (1.2), where  $\alpha$  is an undetermined variational parameter. In Sec. IV the same problem is solved with the trial function that contains two variational parameters. In Sec. V the latter function is used to calculate the exchange-correlation effect. The Appendix gives some integrals of powers of  $z$  times the fourth power of the Airy functions and their derivatives, which are needed to evaluate the variational integral.

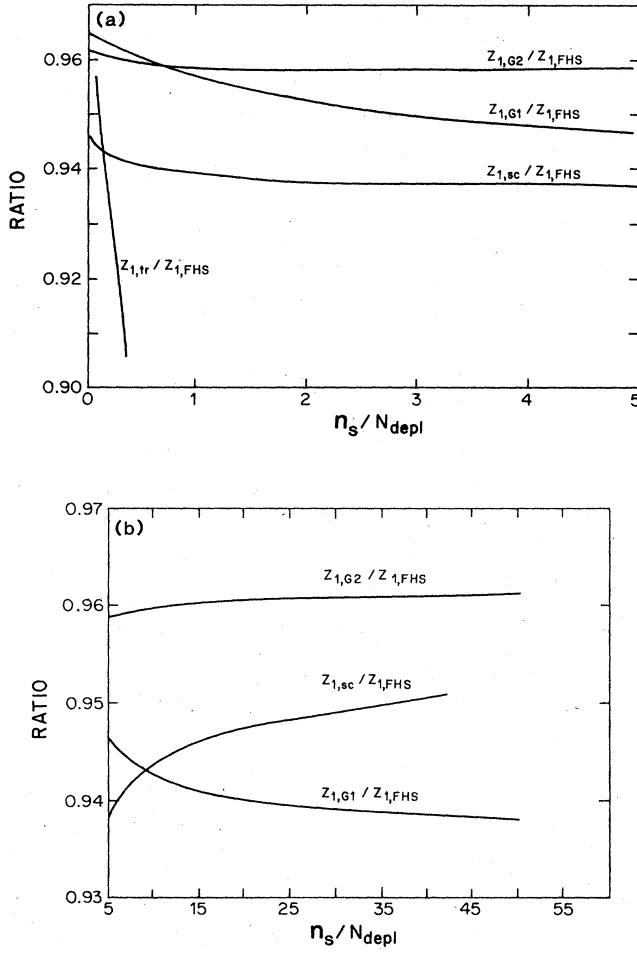


FIG. 2. Ratios of the average electron distances  $Z_{1,sc}$ ,  $Z_{1,tr}$ ,  $Z_{1,G1}$ , and  $Z_{1,G2}$  from the surface to  $Z_{1,FHS}$  as function of  $n_s/N_{depl}$ . Values for  $Z_{1,sc}$  were taken from Ref. 3.

$$\langle E \rangle = -(\hbar^2/2m) \int_0^\infty \xi \frac{d^2 \xi}{dz^2} dz - (2\pi e^2 N/\epsilon) \int_0^\infty (z^2 - 2Lz) |\xi|^2 dz + \frac{1}{2} \int_0^\infty eV_e |\xi|^2 dz. \quad (2.8)$$

Parameters of the trial function are determined from the condition of minimum  $\langle E \rangle$  and the subband energy is found from Eq. (2.7).

### III. EVALUATION OF THE ENERGY WITH THE TRIAL FUNCTION $\xi \sim \text{Ai}(\xi)$

If we take the trial function in the form of Eq. (1.2), but assume that  $\alpha$  is the undetermined variational parameter then

$$V_e(z) = \frac{4\pi n_s}{3\epsilon\alpha} \left[ 2\gamma + \frac{\text{Ai}(\xi)\text{Ai}'(\xi) + 2\xi[\text{Ai}'(\xi)^2 - 2\xi^2\text{Ai}^2(\xi)]}{[\text{Ai}'(-\gamma)]^2} \right]. \quad (3.1)$$

Substituting (3.1) in (2.8) we find

$$\langle \bar{E}(\bar{\alpha}) \rangle = \gamma \bar{\alpha}^2/3 + (16\pi\gamma/3\bar{\alpha}) \left[ \bar{N}_{depl} - \frac{2\bar{N}\gamma}{5\bar{\alpha}} + \frac{3\bar{n}_s}{8} \right]. \quad (3.2)$$

For the relevant integrals of the second power of the Airy

## II. BASIC EQUATIONS

In the region of the two-dimensional electron gas, the charge density is the sum of the ionized-impurity ( $eN$ ) and the electron charge densities:

$$\rho(z) = -e[N + n_s |\xi(z)|^2]. \quad (2.1)$$

Integrating Poisson's equation with the charge density (2.1) yields

$$dV(z)/dz = -F(0+) + (4\pi e/\epsilon)Nz + F_e(z), \quad (2.2)$$

where

$$F_e(z) = (4\pi n_s/\epsilon) \int_0^z |\xi(z')|^2 dz' \quad (2.3)$$

is the part of the total electric field which is proportional to  $n_s$ .

Because the wave function  $\xi(z)$  extends over a distance much less than the depletion-layer width  $L$ , it follows from (2.2) that

$$F(0+) = (4\pi e/\epsilon)(N_{depl} + n_s). \quad (2.4)$$

A second integration of Eq. (2.2) gives the potential

$$V(z) = V(0) + (2\pi eN/\epsilon)(-2Lz + z^2) + V_e(z), \quad (2.5)$$

where

$$V_e(z) = -(4\pi n_s/\epsilon) \left[ \int_0^\infty z |\xi(z)|^2 dz + \int_z^\infty (z-z') |\xi(z')|^2 dz' \right]. \quad (2.6)$$

Substituting Eq. (2.6) into the Schrödinger equation we obtain a single-particle Hartree equation

$$[-(\hbar^2/2m)d^2/dz^2 - eV(z)]\xi(z) = E\xi(z). \quad (2.7)$$

To use the variational principle it is necessary to write the equation for the full energy of the 2DEG. This energy divided by the number of the electrons is given by

functions see Ref. 3 and for the fourth power see the Appendix.

The condition for the minimum  $\langle E(\alpha) \rangle$  gives the equation for  $\alpha$ ,

$$\bar{\alpha}^3 - 8\pi[\bar{N}_{depl} + (3\bar{n}_s/8) - (4\bar{N}\gamma/5\bar{\alpha})] = 0, \quad (3.3)$$

and from Eq. (2.7) we find the bottom-subband energy

$$\tilde{E}_{G1} = (\gamma/3) \{ \tilde{\alpha}^2 + (16\pi/\tilde{\alpha}) [\tilde{N}_{\text{depl}} + (3\tilde{n}_s/4) - (2\tilde{N}\gamma/5\tilde{\alpha})] \}. \quad (3.4)$$

Within the same accuracy as that of Eq. (1.10), we have

$$\tilde{\alpha} = \tilde{\alpha}_{G1} = 2 \left[ \pi \left[ \tilde{N}_{\text{depl}} + \frac{3\tilde{n}_s}{8} \right] \right]^{1/3} - \frac{4\tilde{N}\gamma}{15[\tilde{N}_{\text{depl}} + (3\tilde{n}_s/8)]}, \quad (3.5)$$

$$\tilde{E}_{G1} = \frac{4\pi^{2/3}\gamma[\tilde{N}_{\text{depl}} + (5\tilde{n}_s/8)]}{[\tilde{N}_{\text{depl}} + (3\tilde{n}_s/8)]^{1/3}} - \frac{8\pi^{1/3}\gamma\tilde{N}[\tilde{N}_{\text{depl}} + (\tilde{n}_s/8)]}{15[\tilde{N}_{\text{depl}} + (3\tilde{n}_s/8)]^{5/3}}. \quad (3.6)$$

If we neglect the terms of order  $\lambda$  in  $E_{\text{FHS}}$  [see Eq. (1.11)] and in Eq. (3.6) then the ratio of these energies is

$$\tilde{E}_{G1}/\tilde{E}_{\text{FHS}} = \frac{2}{3} \left[ \frac{2}{9} \right]^{1/3} \frac{\gamma[\tilde{N}_{\text{depl}} + (5\tilde{n}_s/8)]}{[\tilde{N}_{\text{depl}} + (55\tilde{n}_s/96)]} \times \left[ \frac{[\tilde{N}_{\text{depl}} + (11\tilde{n}_s/32)]}{[\tilde{N}_{\text{depl}} + (3\tilde{n}_s/8)]} \right]^{1/3}. \quad (3.7)$$

This ratio is plotted in Fig. 1 as function of  $n_s/N_{\text{depl}}$ . As can be seen,  $E_{G1}$  is less than  $E_{\text{FHS}}$  at all values of  $n_s$ . To compare it with the numeric self-consistent calculation of the  $E_{\text{sc}}$  we plotted the ratio  $E_{\text{sc}}/E_{\text{FHS}}$  using the data tabulated in Ref. 3. Figure 1 shows that our result is only 1.2% larger than the exact result at the larger values of  $n_s$ . In the region  $n_s < 5N_{\text{depl}}$  it diverges from the exact solution by less than 1%.

The values  $Z_{1,G1}$  and  $Z_{2,G1}$  are defined by Eqs. (1.6) where  $\alpha_{\text{tr}}$  must be replaced by  $\alpha_{G1}$ . Ratios  $Z_{1,G1}/Z_{1,\text{FHS}}$  and  $Z_{1,\text{sc}}/Z_{1,\text{FHS}}$  are plotted in Fig. 2 as function of  $n_s/N_{\text{depl}}$ . The difference of these values is close to 2% at low concentration  $n_s$  and it decreases with increasing  $n_s$ , going to 0 at  $n_s/N_{\text{depl}} \simeq 10$ . At larger concentrations it changes sign [see Fig. 2(b)]. We see that both the trial functions (1.2) and (1.8) overestimate the value of  $Z_1$  in the region where the ratio  $n_s/N_{\text{depl}} < 10$  but at larger values  $n_s/N_{\text{depl}}$  we have  $Z_{1,\text{sc}} > Z_{2,G1}$ .

#### IV. ENERGY EVALUATION WITH THE TRIAL FUNCTION $\zeta \sim z^\nu \exp(-az/2)$

In this section we consider the problem of evaluating the energy with a trial function of the form

$$\zeta(z) = \frac{\alpha^{(2\nu+1)/2}}{\Gamma^{1/2}(2\nu+1)} z^\nu \exp(-az/2) \quad (4.1)$$

having two variational parameters  $\nu$  and  $\alpha$ .  $\Gamma(x)$  is the  $\Gamma$  function. The function (4.1) is a generalization of the function (1.8) and it coincides with (1.8) when  $\nu=1$ .

Substituting (4.1) in Eq. (2.8) we have

$$\langle \tilde{E}(\tilde{\alpha}, \nu) \rangle = \frac{\tilde{\alpha}^2}{4(2\nu-1)} + \frac{8\pi\tilde{N}}{\tilde{\alpha}^2} [(\tilde{\alpha}\tilde{L} - \nu - 1)(2\nu+1)] + \frac{4\pi\tilde{n}_s}{\tilde{\alpha}} (2\nu+1)[1-f(\nu)], \quad (4.2)$$

where

$$f(\nu) = \frac{1}{\Gamma(2\nu+2)2^{4\nu+3}} \sum_{k=0}^{\infty} \frac{(k+1)\Gamma(4\nu+k+3)}{2^k\Gamma(2\nu+k+3)}. \quad (4.3)$$

Note that  $f(1) = \frac{5}{16}$ .

The function (4.3) could be written in the form

$$f(\nu) = \frac{\Gamma(2\nu + \frac{3}{2})}{2\pi^{1/2}\Gamma(2\nu+3)} \sum_{k=0}^{\infty} (k+1)A(k), \quad (4.4)$$

where

$$A(0) = 1, \quad A(k) = \frac{4\nu+k+2}{2(2\nu+k+2)} A(k-1). \quad (4.5)$$

The minimum condition  $\partial\langle E(\alpha, \nu) \rangle / \partial\alpha = 0$  gives

$$\tilde{\alpha}^3 - 16\pi(4\nu^2 - 1)[\tilde{N}^*(\nu) + (2\tilde{N}/\tilde{\alpha})(\nu+1)] = 0, \quad (4.6)$$

where

$$\tilde{N}^*(\nu) = \tilde{N}_{\text{depl}} + \frac{1}{2}[1-f(\nu)]\tilde{n}_s.$$

Using Eq. (4.6), Eq. (4.2) could be rewritten

$$\langle \tilde{E}(\tilde{\alpha}, \nu) \rangle = \tilde{\alpha}^2/2(2\nu-1) + (4\pi/\tilde{\alpha})(2\nu+1)\tilde{N}^*(\nu) \quad (4.7)$$

and the expression for energy subband takes the form

$$\tilde{E} = \tilde{\alpha}^2/2(2\nu-1) + (4\pi/\tilde{\alpha})(2\nu+1)[\tilde{N}_{\text{depl}} + \frac{3}{2}\tilde{n}_s(1-f(\nu))]. \quad (4.8)$$

Within the same accuracy as in Eq. (1.10) we find from Eq. (4.6)

$$\tilde{\alpha} = 2[2\pi(4\nu^2 - 1)\tilde{N}^*(\nu)]^{1/3} - 2(\nu+1)\tilde{N}/3\tilde{N}^*(\nu). \quad (4.9)$$

Below we shall neglect the correction term in (4.9). Then substituting  $\alpha$  in Eq. (4.2) we obtain

$$\langle \tilde{E}(\nu) \rangle = [3/(2\nu-1)][2\pi(4\nu^2 - 1)\tilde{N}^*(\nu)]^{2/3}. \quad (4.10)$$

To find the minimum of  $\langle \tilde{E}(\nu) \rangle$  we note that the function  $f(\nu)$  could be approximated by the function

$$f(\nu) = 5(5-\nu)/64 \quad (4.11)$$

in the interval  $\nu=1-1.6$  with an accuracy of 0.6%. Then using (4.11) we find that the minimum of  $\langle E(\nu) \rangle$  occurs for

$$\nu = \nu_m = \frac{1}{4} - \delta + \left[ \delta^2 + \frac{5\delta}{2} + \frac{11}{48} \right]^{1/2}, \quad (4.12)$$

where

$$\delta = \left[ 64N_{\text{depl}} + \frac{39n_s}{2} \right]^{1/2} / 15n_s. \quad (4.13)$$

As can be seen from Eq. (4.12)  $\nu_m \rightarrow \frac{3}{2}$  when  $n_s/N_{\text{depl}} \rightarrow 0$  and  $\nu_m \rightarrow 1.223$  when  $n_s/N_{\text{depl}} \rightarrow \infty$ . The

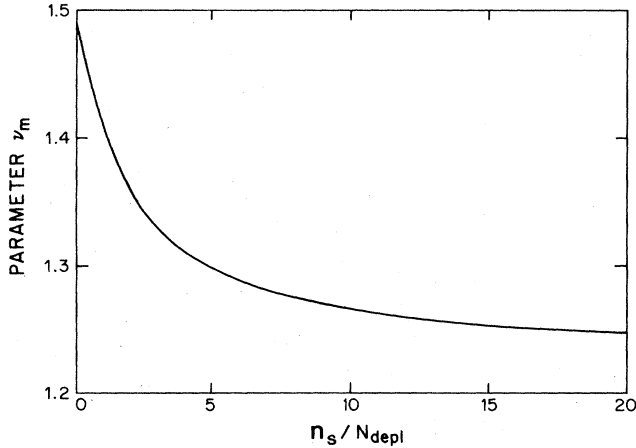


FIG. 3. Dependence of the parameter  $\nu_m$  in the wave function (4.1) on the ratio  $n_s / N_{\text{depl}}$ .

dependence of  $\nu_m$  on the ratio  $n_s / N_{\text{depl}}$  is displayed in Fig. 3.

From Eq. (4.8) it follows that the bottom-subband energy is given by

$$\begin{aligned} \tilde{E} = \tilde{E}_{G2} = 3 \frac{[2\pi(4\nu_m^2 - 1)\tilde{N}^*(\nu_m)]^{2/3}}{2\nu_m - 1} \\ \times \left[ 1 + \frac{\tilde{n}_s [1 - f(\nu_m)]}{3\tilde{N}^*(\nu_m)} \right]. \end{aligned} \quad (4.14)$$

The values  $Z_1$  and  $Z_2$  are equal in this case

$$\begin{aligned} Z_1 = Z_{1,G2} = (2\nu_m + 1)/\alpha, \\ Z_2 = Z_{2,G2} = 2(\nu_m + 1)(2\nu_m + 1)/\alpha^2. \end{aligned} \quad (4.15)$$

Ratios  $E_{G2}/E_{\text{FHS}}$  and  $Z_{1,G2}/Z_{1,\text{FHS}}$  are plotted in Fig. 1 and Fig. 2. At low values of  $n_s / N_{\text{depl}}$  a better result for the energy is obtained when we used Airy trial function; however, in the whole interval of the  $n_s$  the difference between them does not exceed 1.5%. The value  $Z_{1,G2}$  is 2% larger than the corresponding exact value  $Z_{1,\text{sc}}$ .

## V. EXCHANGE-CORRELATION ENERGY

In this section we calculate the exchange-correlation correction to the energy by using the local-density-functional approximation.<sup>9-11</sup> This method has been successfully used by a number of authors<sup>12-14</sup> in the numerical calculations of the subband energy.

The exchange-correlation potential energy  $V_{\text{ex}}(z)$  has been parametrized by a number of authors. We will use the analytic parametrization proposed by Hedin and Lundqvist:<sup>15</sup>

$$\tilde{V}_{\text{ex}}(z) = V_0 [y + 0.7734 \ln(1 + y)], \quad (5.1)$$

where

$$V_0 = 2/7(12\pi^2)^{1/3}, \quad (5.2)$$

$$y(z) = 21(4\pi R_B \tilde{n}_s |\zeta(z)|^2/3)^{1/3}. \quad (5.3)$$

In the practical range of the parameter values the potential  $V_{\text{ex}}(z)$  can be considered as perturbation to the main Hartree potential. Therefore we can calculate a change of the energy level in the first-order perturbation theory using the variational wave function as the wave function of the zero approximation. Then the exchange-correlation correction of the energy is

$$\Delta \tilde{E}_{\text{ex}} = \int_0^\infty \tilde{V}_{\text{ex}}(z) |\zeta(z)|^2 dz. \quad (5.4)$$

The function  $y(z)$  goes to zero on the both sides of the integration interval as  $|\zeta(z)|^{2/3}$ , i.e., considerably slower than  $|\zeta(z)|^2$ . In the main region of the integration the function  $y(z)$  is much larger than unity. Therefore we can neglect the unity in comparison with  $y(z)$  under the sign of the logarithm in  $V_{\text{ex}}(z)$ . The numerical calculation shows that the error of this approximation does not exceed 3%. Using the wave function (4.1) we obtain

$$\begin{aligned} \Delta \tilde{E}_{\text{ex}} = V_0 \left[ \left( \frac{3}{4} \right)^{8\nu_m/3} \frac{\Gamma(8\nu_m/3)}{\Gamma(2\nu_m)} Q \right. \\ \left. + 0.7734 \left[ \ln Q - \frac{2\nu_m + 1}{3} \right. \right. \\ \left. \left. + \frac{2\nu_m}{3} \Psi(2\nu_m + 1) \right] \right], \end{aligned} \quad (5.5)$$

where

$$Q = 21[4\pi \tilde{\alpha} \tilde{n}_s / 3\Gamma(2\nu_m + 1)]^{1/3} \quad (5.6)$$

and  $\Psi(\gamma)$  is the logarithmic derivative of the  $\Gamma$  function.

In Fig. 4 the ratio  $|\Delta E_{\text{ex}}| / (E_{G2} + \Delta E_{\text{ex}})$  is plotted as function of  $n_s / N_{\text{depl}}$  for  $N_{\text{depl}} = 10^{10} \text{ cm}^{-2}$ , electron effective mass  $m = 0.07m_0$  and dielectric constant  $\epsilon = 13$ . As can be seen the importance of the exchange-correlation correction decreases with increasing surface concentration  $n_s$ . In Fig. 5 we plotted  $\Delta E_{\text{ex}}$  as the function of the ratio  $n_s / N_{\text{depl}}$  for the same values of the parameters as for Fig. 4. One of the curves is plotted for  $\nu_m = 1$ , which corresponds to the Fang-Howard wave function. It gives the

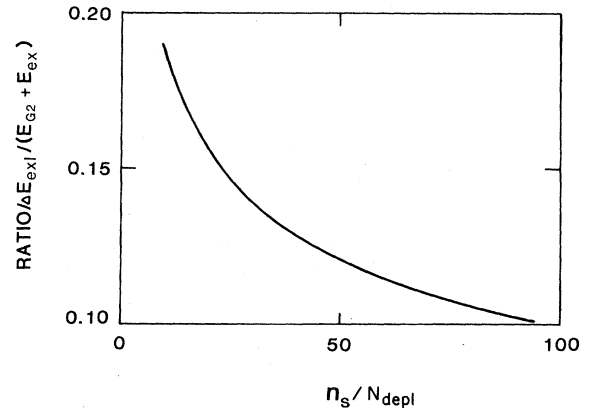


FIG. 4. Relative value of the exchange-correlation correction as a function of  $n_s / N_{\text{depl}}$ .

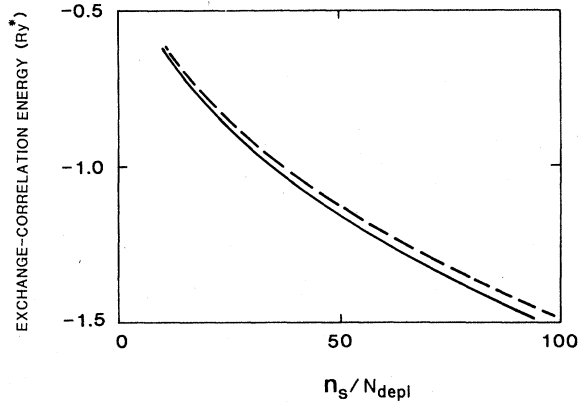


FIG. 5. Exchange-correlation correction of the energy level as the function of  $n_s/N_{\text{depl}}$ .  $Ry^*$  is the effective Rydberg, 5.6 meV. Solid curve,  $\nu = \nu_m$ ; dashed curve,  $\nu = 1$ .

smaller absolute value of the  $\Delta E_{\text{ex}}$ , and therefore the difference in the values of the energies that are calculated by these functions increases.

## VI. CONCLUSION

As can be seen from the above, both proposed solutions lead to fairly close results. From a practical point of view one should prefer the second solution [i.e., the case described by Eq. (4.1)] because the Fourier transform of this wave function can be expressed in a simple analytical form

$$\begin{aligned} \xi(q) &= \int_0^\infty \xi(z) \exp(-iqz) dz \\ &= \frac{2^{\nu+1} \alpha^{\nu+1/2} \Gamma(\nu+1)}{[\Gamma(2\nu+1)]^{1/2} (\alpha+2iq)^{\nu+1}}. \end{aligned}$$

This allows one to use it in quantum-mechanical calculations.

The dependence of the parameter  $\nu_m$  on  $n_s/N_{\text{depl}}$  shown in Fig. 3 demonstrates that the deviation of  $\nu_m$  from unity plays an important role. This ratio for the inversion layer at the semiconductor/insulator interface may be close to unity. In this case  $\nu_m$  approaches 1.5 which should substantially affect the probability of processes with the momentum change  $q$  larger than  $\alpha$ . For the two-dimensional electron gas in AlGaAs-GaAs heterostructures the inequality  $n_s \gg N_{\text{depl}}$  is practically always fulfilled. In this case  $\nu_m \simeq 1.2$  and, hence the corrections related to the use of the function (1.8) are less important. In spite of this, the calculation of the exchange-correlation energy shows that, at a large value of the ratio  $n_s/N_{\text{depl}}$ , the correction mentioned above is still important.

## ACKNOWLEDGMENTS

The author is indebted to M. S. Shur for a discussion and to C. H. Hyun for assistance in preparing the manuscript. This work has been partially supported by Microelectronics and Information Sciences Center at the University of Minnesota.

## APPENDIX: INTEGRALS OF AIRY FUNCTIONS

In connection with the calculation of the average energy of the electron gas for the Airy trial function we note the following indefinite integrals:

$$\int x \text{Ai}^4(x) dx = [3x^2 \text{Ai}^4 + 3(\text{Ai}')^4 + 2 \text{Ai}^3 \text{Ai}' - 6x \text{Ai}^2 (\text{Ai}')^2] / 8, \quad (\text{A1})$$

$$\int x^2 \text{Ai}^4(x) dx = [-7 \text{Ai}^4 + 12x^3 \text{Ai}^4 + 28x \text{Ai}^3 \text{Ai}' - 24x^2 \text{Ai}^2 (\text{Ai}')^2 - 12 \text{Ai} (\text{Ai}')^3 + 12x (\text{Ai}')^4] / 64, \quad (\text{A2})$$

$$\int x \text{Ai}^2(x) (\text{Ai}')^2(x) dx = [-3 \text{Ai}^4 / 4 - x^3 \text{Ai}^4 + 3x \text{Ai}^3 \text{Ai}' + 2x^2 \text{Ai}^2 (\text{Ai}')^2 + \text{Ai} (\text{Ai}')^3 - x (\text{Ai}')^4] / 16, \quad (\text{A3})$$

$$\int \text{Ai}^2(x) (\text{Ai}')^2(x) dx = [-x^2 \text{Ai}^4 + 2 \text{Ai}^3 \text{Ai}' + 2x \text{Ai}^2 (\text{Ai}')^2 - (\text{Ai}')^4] / 8, \quad (\text{A4})$$

$$\int x \text{Ai}(x) (\text{Ai}')^3(x) dx = (\text{Ai}')^4 / 4, \quad (\text{A5})$$

$$\int \text{Ai}^3(x) \text{Ai}'(x) dx = \text{Ai}^4 / 4, \quad (\text{A6})$$

where  $\text{Ai} = \text{Ai}(x)$  and  $\text{Ai}' = \text{Ai}'(x)$  denotes the derivative of  $\text{Ai}$  with respect to  $x$ .

<sup>1</sup>F. F. Fang and W. E. Howard, Phys. Rev. Lett. **16**, 797 (1966).

<sup>2</sup>J. A. Pals, Phys. Lett. A **39**, 101 (1972).

<sup>3</sup>F. Stern, Phys. Rev. B **5**, 4891 (1972).

<sup>4</sup>C. B. Duke, Phys. Rev. **159**, 632 (1967).

<sup>5</sup>J. A. Appelbaum and G. A. Baraff, Phys. Rev. B **4**, 1235 (1971); **4**, 1246 (1971).

<sup>6</sup>G. A. Baraff and J. A. Appelbaum, Phys. Rev. B **5**, 475 (1972).

<sup>7</sup>B. Vinter, Appl. Phys. Lett. **44**, 307 (1983).

<sup>8</sup>Handbook of Mathematical Functions, edited by M.

Abramowitz and I. A. Stegun (U. S. GPO, Washington, D. C., 1964), Chap. 10.

<sup>9</sup>P. Hohenberg and W. Kohn, Phys. Rev. **136**, B864 (1964).

<sup>10</sup>W. Kohn and L. J. Sham, Phys. Rev. **140**, A1133 (1965).

<sup>11</sup>L. J. Sham and W. Kohn, Phys. Rev. **145**, 561 (1966).

<sup>12</sup>T. Ando, Phys. Rev. B **13**, 3468 (1976).

<sup>13</sup>S. Das Sarma and B. Vinter, Phys. Rev. B **23**, 6832 (1981); **26**, 960 (1982); **28**, 3639 (1983).

<sup>14</sup>F. Stern and S. Das Sarma, Phys. Rev. B **30**, 840 (1984).

<sup>15</sup>L. Hedin and B. I. Lundqvist, J. Phys. C **4**, 2064 (1971).